Sustainable and Safe Dams Around the World – Tournier, Bennett & Bibeau (Eds)

The redesign of a plunge pool slab for a temporary diversion due to dynamic pressures

R. Haselsteiner
Bjoernsen Consulting Engineers, Koblenz, Germany

A. Trifkovic
Fichtner GmbH & Co. KG, Stuttgart, Germany

ABSTRACT: The Bujagali HEPP is a runoff-river project located on the White Nile in Uganda. The project was commissioned in the year 2012 and hosts five 50 MW Kaplan turbines. The principle design shows a gated spillway, an emergency syphon spillway, the powerhouse and the left, center and right embankment dams. The Nile River shows two stream sections at the project location. Hence, the construction works were executed during two diversion phases. The right bay of the gated spillway is equipped with a flap gate. This bay discharges after diversion end into a tailwater plunge pool. For the stability analysis of the base slab the assumption of a hydraulic pressure distribution underneath the slab was required. The resulting load conditions and pore pressure results led to a change of the design in favour of the application of vertical anchors. Most up-to-date findings in research at the time of redesign also led to a re-evaluation of the applicable safety factors.

RÉSUMÉ: Le HEPP de Bujagali est un projet situé le long du Nil Blanc en Ouganda. Le projet a été mis en service en 2012 et se compose de cinq turbines Kaplan de 50 MW. La conception principale montre un déversoir à porte, l'évacuateur d'urgence à siphon, la centrale électrique et les barrages gauche, central et droit. Le Nil montre deux sections de cours d'eau à l'emplacement du projet. Voilà pourquoi ces travaux de construction ont été réalisés lors de deux phases de détournement. La baie de droite de l'évacuateur est équipée d'une protection antiretour. Cette baie se décharge après déviation dans un bassin de rétention. Les conditions de poids et de pression qui en résultent favorisent l'application d'ancrages verticaux et une dalle fortifié. Les résultats d'une recherche avancée lors du planning du réaménagement, ont donc conduit à une réévaluation des facteurs de sécurité applicables.

1 THE PROJECT AND INTRODUCTION

The Bujagali Hydroelectric Power Plant (HEPP) is located in the southern area of Uganda on the Victoria Nile River, approximately 8 km downstream of the town of Jinja. In that area, the river is divided in two branches around the Dumbbell Island. The dam axis crosses the river at Dumbell Island, the Hydro Power Plant will be located in the left branch of the river. The general layout of the project is given in Figure 1.

Bujagali Energy Limited (BEL), Uganda, is the owner of the 255 MW Hydroelectric Power Plant. The main works of the Bujagali Hydroelectric Power Project are embankment dams with a maximum height of 30 m (left, central, right), a gravity dam, a powerhouse, a gated spillway, and a siphon spillway. The crest elevation of the embankment dam sections and of the concrete structures is at 1,114.5 m.a.s.l. The embankment dams are a clay core sealed rockfill dam.

During the 2nd diversion phase a design discharge of 2,250 m³/s has to be conducted through two fully opened radial gates and a temporary bay equipped with a flap gate. Each radial gate

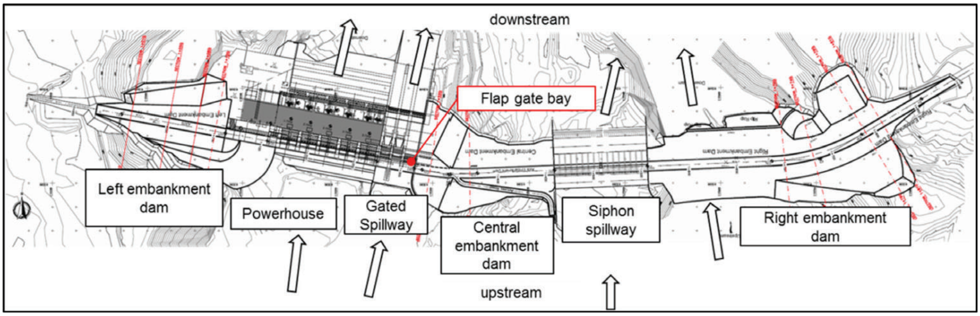

Figure 1. Site map of the project area with flap gate bay

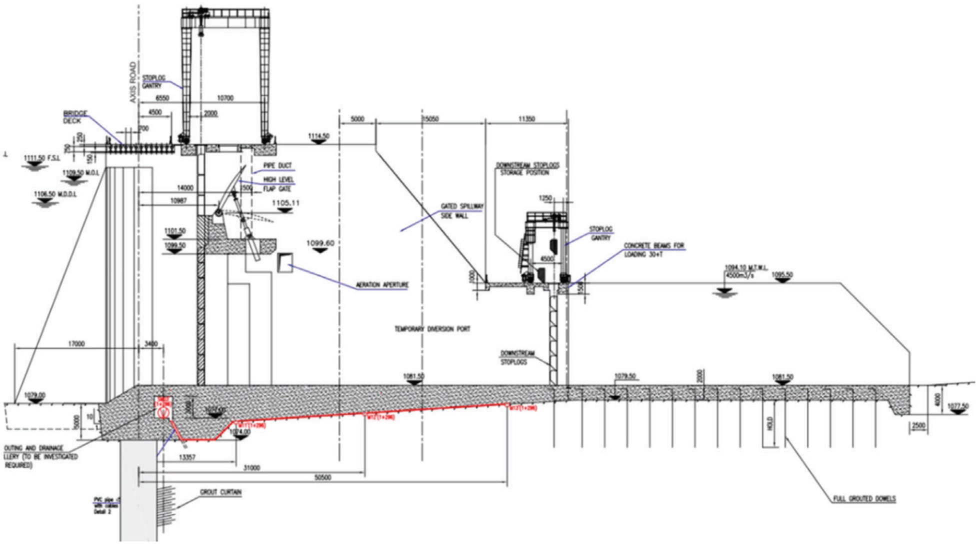

Figure 2. Section through the flap gate spillway and site map

bay has a width of 9.5 m and a fully opened height of 10.5 m. The third bay with the flap gate that is used during 2nd stage diversion is a rectangular section with a width of 12 m. This temporary opening shall be closed by a plug after the 2nd diversion stage is completed. A cross section through the flap gate diversion structure is given in Figure 2.

It is to be mentioned that the bottom slabs of the spillway structures are located at an elevation of 1081.5 m.a.s.l. The flap gate is located at an elevation of about 1,105 m.a.s.l. This results in a considerable height difference between the upstream and downstream water levels.

2 FUNDAMENTALS OF PLUNGE POOLS DESIGN

2.1 *Fundamental considerations of plunge pools*

Typical plunge pool systems are located behind overflow structures of (double curvature) arch dams like is shown in the sketch of Figure 3. A concrete lined plunge basin is one among other possibilities of energy dissipation such as natural scour pools or weir downstream pools (May & Willoughby, 1991). With decreasing structure and reservoir height and rising tailwater depth the systems moves toward a drop or flow structure. The change-over appears fluently. Nevertheless, stilling basins of river weirs have to bear comparable load conditions as arch

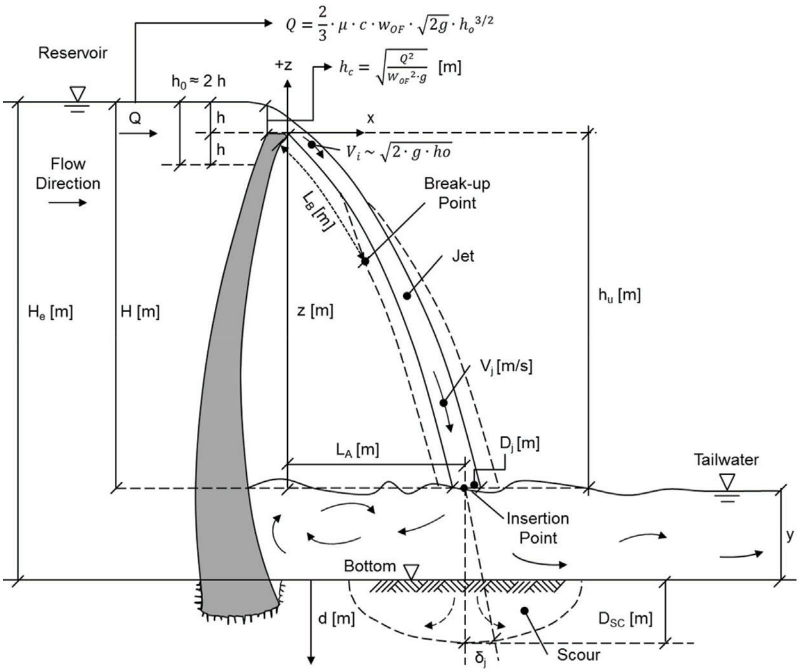

Figure 3. Hydraulic parameters of typical plunge pool systems with an overflow crest (sketch)

dam plunge basins although having different hydraulic circumstances and usually lower hydraulic heads. In the sketch shown in Figure 3 the required parameters (in total 22 parameters) which are essential for the determination of dynamic pressures are indicated.

Plunge basins or pools are a very economical way for providing energy dissipation if tolerable scour is pronounced. If the thread of scouring leads to an unpredictable risk special protection measures have to be taken such as liners consisting of concrete slabs or steel.

The impact on the subsoil is dominated by the load parameters q [m³/s/m] and the fall height H [m], that is equal to the difference between reservoir and tailwater level $H = H_e - Y$, and the material resistance that is often expressed by a characteristic grain size diameter d [m]. Of course for rock foundation d [m] is just a crutch. But research works are already propagating scouring rock models (Bollaert, 2005).

Important influence is exerted by the tailwater depth Y [m] or the ratio of tailwater depth to jet diameter D_J [m] at impingement. This ratio represents the "water cushion" that is absorbing the inserted jet energy. Moreover the different flow conditions of the flow jet should be respected. As it is stated below aerated jets cause lower pressures than others. The degree of aeration can be respected by the ratio of break-up length LB [m] and fall height H [m]. The break-up points indicates the state whereas maximum aeration is reached and a compact jet flow is changing to discrete water droplets. The distance from overflow kerb to the intrusion point is called L_A [m] and is important for the estimation of scour extents or of the length of a protection structure.

For the description and explanation of all the mentioned parameters the authors would like to forward to the specific literature (Bollaert, 2004, Bollaert & Schleiss, 2003, 2005; Castillo, 2006; Castillo & Castillo, 2016; Puertas & Dolz, 2005).

2.2 *Hydraulic load distribution onto base slabs in plunge pools*

The occurring pressures on concrete slabs on the bottom floor of plunge pools are composed of the three components (a) static hydraulic pressure caused by under seepage flow, (b) mean dynamic pressure caused by the jet impact, and (c) fluctuating dynamic pressure caused by turbulent flow.

All three pressure loads have to be superposed for obtaining the actual load distribution. A system sketch presenting typical loading conditions for concrete floor slabs/liners caused by rectangular flow jets is given by Figure 4.

Mean dynamic pressures above and underneath the liner balance each other out. The hydraulic static loading conditions result in a triangular pressure distribution according to the hydraulic boundary conditions. With rising thickness of the concrete liner and a deeper foundation elevation also the static pressure underneath is increasing. Therefore, the design of a concrete base slab is an iterative process analysis the effect of design adaptations on the pressure conditions.

Sealings and/or drainages lead to a diminution of the hydraulic pore pressure in the subsoil. This effect can be respected by multiplying the hydraulic height difference by a diminution factor ξ. For a total reduction of the reservoir head this factor becomes zero when backwater influence can be excluded, too. For practical use values of $\xi = 0.30$ to 0.90 are achievable in practice.

Mean dynamic pressures caused by the jet impact cancel each other out regarding the force onto base slab whilst fluctuating dynamic pressure may exhibit an uplift force. In opposite to static hydraulic pressures these pressures are subject to the dynamic evolution of the hydraulic jet impact and the fluctuating pressure may also show uplift characteristics.

2.3 *Equations and analyses*

For the empirical-analytical determination of the hydraulic (static and dynamic) pressures underneath the concrete base slab within the stilling basin or plunge pool some selected basic

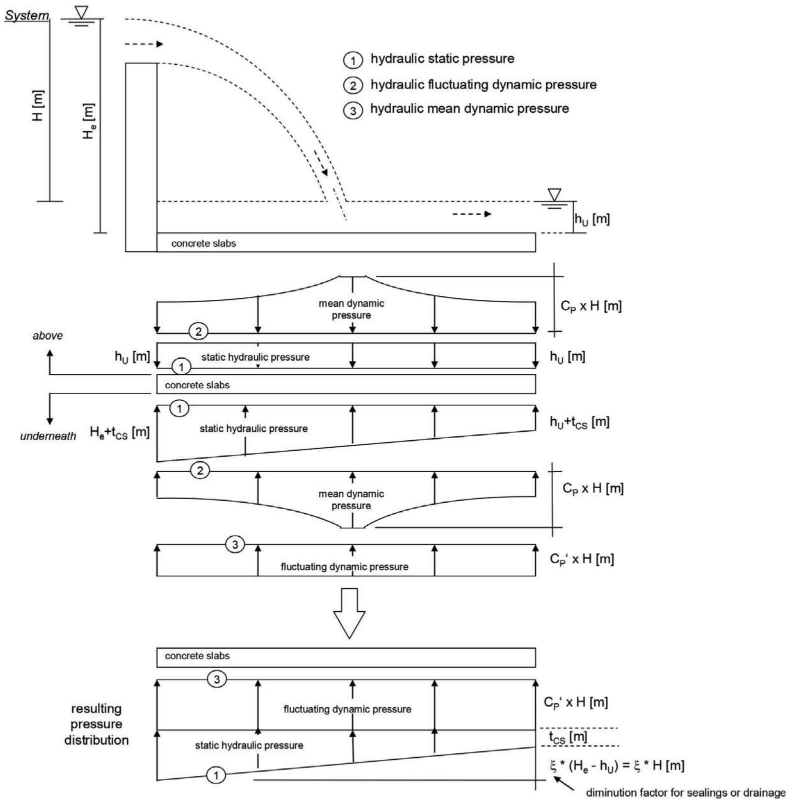

Figure 4. Simplified loading condition model for base slabs of plunge pools due to hydraulic pressures

equations are given below. First, the diameter at the insertion point D_j [m] is required for the estimation of dynamic pressures onto the bottom of plunge pools. Equation (1) is taken from Castillo (2006) and it provides a estimation of D_J [m] including both the solid core jet and the aerated flow width:

$$D_J = \frac{q}{\sqrt{(H_e - Y) \cdot 2 \cdot g}} + 4 \cdot \varphi \cdot \sqrt{2 \cdot h_0} \cdot \left(\sqrt{H_e - Y} - \sqrt{2 \cdot h_0}\right) \quad (1)$$

where D_J = jet diameter at intrusion point [m]; q = specific discharge [$m^3/(s*m)$]; φ = turbulence parameter [-]; H_e = reservoir level/water height [m]; Y = tailwater level/height [m]; h_0 = overflow height [m].

$$\varphi = 1.07 \cdot T_U^* \quad (2)$$

where T^*_U = turbulence intensity [-].

The turbulence intensity T_U* for rectangular flows is defined (Castillo, 2006) as follows in Equation (3):

$$T_U^* = \frac{q^{0.43}}{\frac{14.95 \cdot g^{0.50}}{K^{1.22} \cdot C_d{}^{0.19}}} \approx \frac{q^{0.43}}{50} \quad (3)$$

where C_d = overflow coefficient [-]; K = turbulence coefficient [-].

For conservative assumptions K = 0.85 can be used (Castillo, 2006), even though model or prototype data will probably grant more precise results and probably lower values. The constant C_d = 2.1 is a simple overflow parameter considering overflow spillways and is commonly used.

$$q = 2/3\mu \cdot \sqrt{2 \cdot g} \cdot h_0{}^{3/2} = 2.95 \cdot \mu \cdot h_0{}^{3/2} \quad (4)$$

where μ = overflow parameter after Poleni [-].

Setting equation (2), (3) and (4) to Equation (1) results in following expression:

$$D_J = \frac{2.95 \cdot \mu \cdot h_0{}^{3/2}}{\sqrt{(H_e - Y) \cdot 2 \cdot g}} + 4 \cdot \frac{\left(2.95 \cdot \mu \cdot h_0{}^{3/2}\right)^{0.43}}{50} \cdot \sqrt{2 \cdot h_0} \cdot \left(\sqrt{H_e - Y} - \sqrt{2 \cdot h_0}\right) \quad (5)$$

In Equation (5) the jet diameter D_J can be estimated by only four parameters, H_e, Y, μ, and h_0. The overflow parameter μ [-] can be assumed as constant and can be set to μ = 0.70 for overflow spillways with a relative well shaped ogee overflow crest.

For the determination of the pressure distribution location of the free jet insertion point needs to be determined, e.g., by utilizing the approach of Hager & Vischer (1995), which provides the horizontal distance L_A (compare Figure 3).

As aforementioned in section 3.2 the total pressure is composed by the seepage pore water pressure, the mean dynamic pressure and the fluctuating dynamic pressure. The seepage pore water pressure distribution results from a seepage analysis or from simple assumptions regarding the pressure distribution in consideration of the upstream and downstream water heads. The mean dynamic pressures are given are defined by following equation:

$$C_P = \frac{(H_e - Y)}{\frac{v_J{}^2}{2 \cdot g}} \quad (6)$$

where C_P = mean dynamic pressure coefficient [-]; v_J = jet velocity [m/s].

As can be seen in Figure 6 the values for CP are varying from 0.20 up to 1.0. Focusing on the range of small values of Y/D_J the maximum pressure at the bottom of the plunge pool may reach the maximum available head (H_e-Y) (C_P = 1.0).

The analytical solution for C_P provides a maximum of C_P = 0.85. Even with a raising aeration effect the mean pressure decline, which may be respected by consideration of the ratio between the break-up length L_B [m] and (H_e-Y). The expression (H_e-Y) is often simply called falling height H_F.

Design C_P-values can be taken from the diagrams in literature (Castillo, 2006; Castillo & Carrillo, 2016; Bollaert & Schleiss, 2003; Ervine et al., 1997). As mentioned an analytical approach is provided by Bollaert & Schleiss (2003). Depending on the ratio Y/D_J values for C_P [-] can be determined as follows:

$$C_P = 38.4 \cdot (1 - \alpha_J)^{1.345} \cdot \left(\frac{D_J}{Y}\right)^2 \tag{7}$$

where a_J = air concentration at intrusion point; for Y/D_J > 4 to 6 (developed jets).

$$C_P = 0.85 \tag{8}$$

for Y/D_J < 4 to 6 (core jets).

The hydrodynamic pressures are expressed by the fluctuating dynamic pressure coefficient C_P'. The range for C_P' reaches from C_P' = 0.0 to 0.4. Maximum fluctuating dynamic pressure values can exceed the mentioned limit of C_P' = 0.4 (see Figure 7).

In Bollaert & Schleiss (2003) an analytical solution for the determination of the fluctuating dynamic pressure coefficient C_P' [-] is given as follows:

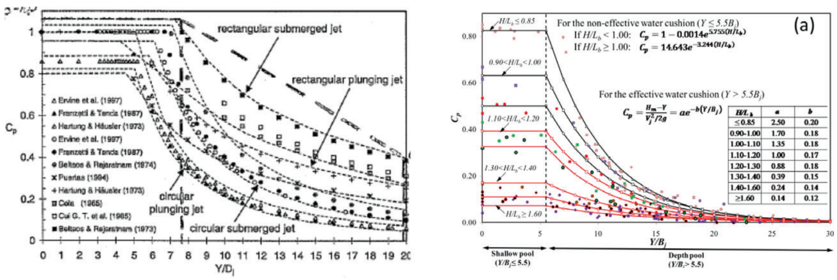

Figure 6. Mean dynamic pressure coefficient CP (left: Bollaert & Schleiss, 2003; right: Castillo & Carrillo, 2016)

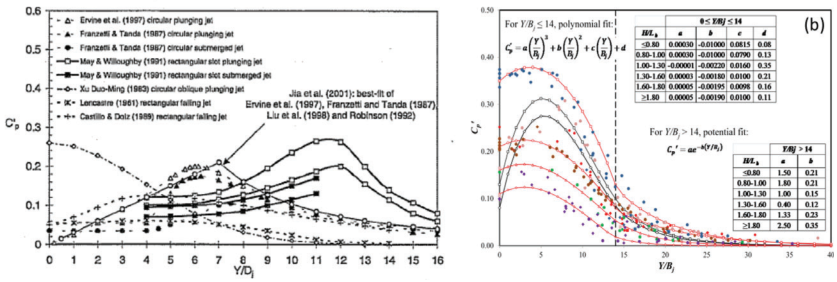

Figure 7. Fluctuating dynamic pressure coefficients using the ratio Y/D_J (left: Bollaert & Schleiss, 2003; right: Castillo & Carrillo, 2016)

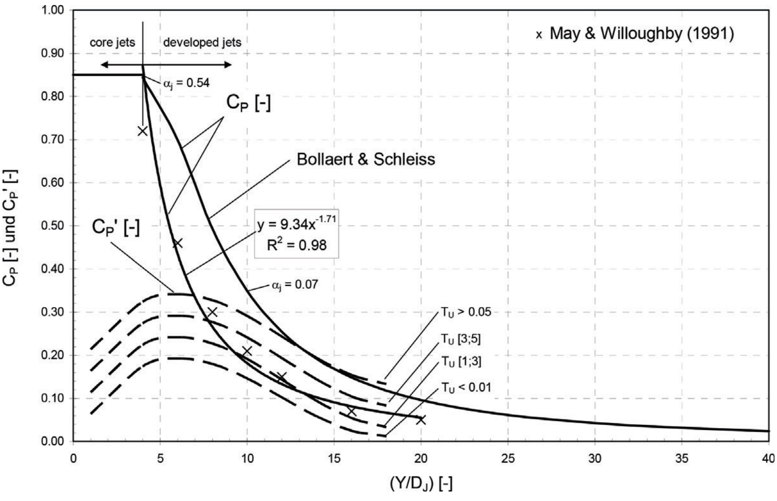

Figure 8. Mean and fluctuating dynamic pressure coefficients using the ratio Y/D_J

$$C_P{}' = a_1 \cdot \left(\frac{D_J}{Y}\right)^3 + a_2 \cdot \left(\frac{D_J}{Y}\right)^2 + a_3 \cdot \left(\frac{D_J}{Y}\right)^1 + a_4 \tag{9}$$

Determination and assumptions for the air concentration are difficult. The effect of the air intrusion onto the pressure behaviour is strongly decreasing for values of $Y/D_J > 4$. Early results of May & Willoughby (1991) affirm the given hints for estimating mean pressure values. A graph respecting data from May & Willoughby (1991) is added to Figure 8. It may provide not as conservative values as Bollaert & Schleiss (2003) do for $Y/D_J > 4$.

The transverse distribution of pressure values are given by Equation 4 5 (after Hager & Vischer, 1995). The literature referred to in Hager & Vischer (1995) do not regard the pressure coefficients but absolute pressure values. As equation (10) simply presents the pressure distribution in y-direction transversal to flow direction the transfer usage to the mentioned pressure coefficient should be possible either.

$$\frac{C_{P,trans}}{C_{P,\max}} = e^{\left(-0.023 \cdot \left(\frac{y}{Y}\right)^2\right)} \tag{10}$$

where $C_{P,trans}$ = transversal dynamic pressure coefficient [-]; $C_{P,max}$ = maximum dynamic pressure coefficient [-]; y = transversal distance from jet intrusion axis [m].

3 LOAD CASES AND DESIGN PARAMETERS

The hydraulic loads due to jet impact were defined according to Table 1. The damping influence of effects such as aeration, turbulence and other influencing effects were assumed conservatively. For the consideration of buoyancy of a plunge pool bottom concrete liner mean dynamic pressure due to jet impact outweigh itself. Thus, effective pressure loads result from fluctuating dynamic hydraulic pressures and static hydraulic pressures. Drainage facilities in combination with a grout curtain lead to a pressure reduction underneath base slabs. The pressures need to be determined in order to design eventually required rock anchoring. The foundation rock is quite weak so that the base slab is considered to be required to avoid uncontrolled scouring.

Table 1. Defined load cases for the design of the plunge pool.

No.	Load Case (LC)	Water loads	Q_{FG}*** [m³/s]	Reservoir water level [m.a.s.l.]*	Tailwater Level [m.a.s.l.]**	Type
LC 1	Normal Operation	TO1	300.00	1,111.50	1,089.60	Normal
LC 2	Minimum flow at Minimum Operating Level	MIF	300.00	1,109.50	1,086.50	Exceptional
LC 3	Standard Project Flood	SPF	300.00	1,111.50	1,092.00	Exceptional
LC 4	Maximum Water Level and maximum discharge	P.M.F./ MIF	400.00	1,112.00	1,094.10	Extreme

* Overflow crest level at 1,105.10 m.a.s.l.
** Plunge pool bottom flow level at 1,081.50 m.a.s.l.
*** FG = flap gate

Table 2. Determined parameters of the plunge pool system (part 1)

No.	q [m³/s/m]	H [m]	h_0 [m]	Y [m]	L_B [m]	H/L_B [-]	h_c [m]	T_U* [-]	D_J [m]	h_U [m]	ξ [-]
LC 1	25	21.9	6.4	8.1	16.81	1.30	4.0	0.08	3.1	15.5	0.67
LC 2	25	23.0	4.4	5.0	16.81	1.37	3.0	0.08	2.0	18.6	0.67
LC 3	25	19.5	6.4	10.5	16.81	1.16	4.0	0.08	2.8	13.1	0.67
LC 4	33	17.9	6.9	12.6	18.43	0.97	4.8	0.09	2.7	11.0	0.67

Table 3. Determined parameters of the plunge pool system (part 2)

No.	z [m]	Z [-]	Z_U [-]	X [-]	LA [m]	w [m]	w/h_c [-]	δ_J [°]	Y/D_J [-]	C_P [-]	C_P' [-]
LC 1	15.5	3.88	3.88	4.2	16.8	23.6	5.90	63	2.61	0.85	0.29
LC 2	18.6	6.20	6.20	5.2	15.6	23.6	7.87	68	2.50	0.85	0.28
LC 3	13.1	3.27	3.27	3.9	15.6	23.6	5.90	63	3.75	0.85	0.32
LC 4	11.0	2.29	2.29	3.2	15.4	23.6	4.92	61	4.67	0.70	0.33

Concluding four load cases were defined considering different upstream and downstream water levels whilst the discharge over the flap gate varies from Q_{FG} = 300 to 400 m³/s (Table 1). The required hydraulic and geometric parameters of the plunge pool system which enable to define the pore water pressure distribution beneath the slabs were determined for the different load cases as shown in Table 2 and Table 3.

4 RESULTS

The resulting hydraulic pressures are given in Figure 9. At the section plane of the grouting/drainage gallery the potential reduction was assumed to be one third of the maximum potential head. Thus, the diminution factor was set to ξ = 0.67. At all geometric changes of the foundation slab reference points P were defined (P1 to P8). Additionally, the potential distribution was assumed to have a linear decline from the grout curtain to the end of the concrete liner approx. 102.25 m downstream of the inflow section. Although a grout curtain inclusive drainage drillings were taken into consideration in the design the hydraulic pressure may show quite large values which results in the necessity for anchoring. Due to an unsymmetrical load distribution the concrete slabs have to be designed also for bending loads.

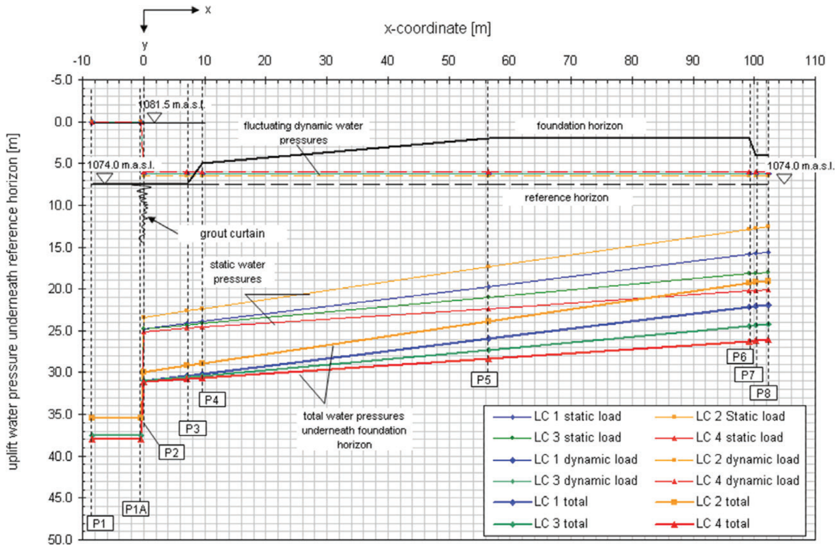

Figure 9. Load figures regarding hydraulic pressure loads on plunge pool liner (pressure on reference horizon) – without box drains – grout curtain and drainage full function

Concerning the relatively slim construction of the concrete liner measures such as anchoring and/or the application of box drains were investigated as it is shown in Figure 10.

For a better understanding of the pressure distribution in Figure 4 the uplift pressures regarding a reference horizon at a level of 1,074.0 m.a.s.l was added. Hereby, the assumed linear decrease of the uplift water pressure can be seen. According to the load cases the net pressures reach peaks upstream the grout curtain and drainage section and after the decrease of the thickness of the bottom liner at x-coordinates greater than 10 m.

As mentioned the uplift pressures reach values that evokes the necessity of anchoring. For a first estimation of necessary anchor lengths some assumption were implemented. The effective

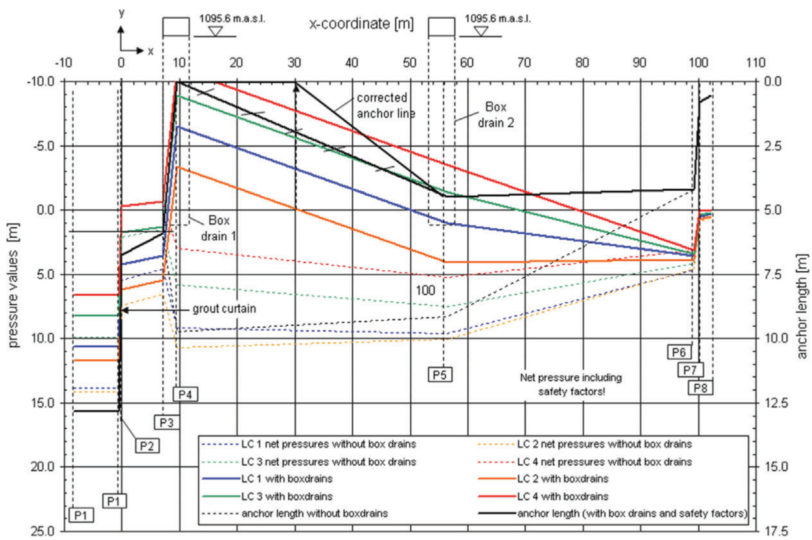

Figure 10. Load figures regarding hydraulic pressure loads on plunge pool liner (net pressures and anchor length) – with box drains – grout curtain and drainage full function

radius of an anchor should be about 1.5/2 = 0.75 m. The effective length of an anchor is 2/3 of the whole anchor length.

In Figure 9 and 10 the net pressure for the load cases mentioned defined in Table 1 are given. Additionally the necessary anchor length due to the maximum pressure which occurs in load case 2 is shown in the graph. The anchor lengths exceed 10 m upstream the grout curtain section and reach nearly 10 m from x-coordinates 10 to 55 m downstream. Generally the anchor lengths for the mentioned load cases are very high.

An alternative is to apply box drains at some sections. As seen in Figure 10 the influence of two box drains at x-coordinates 10 m (P4) and 55 m (P5) was investigated. The maximum uplift pressure can be limited to 14.10 m in this sections assuming the exit point of the box drains at an elevation of 1095.6 m.a.s.l. (= maximum tailwater level + freeboard = 1,094.1 m. a.s.l + 1.5 m). The effects are significant downstream the grout curtain section. There the anchor length can be reduced to 40 % of the situation without.

The application of safety factors in hydraulic design is discussed controversially within the engineering society. E.g. given, Bollaert (2004) refers to amplification factors, which reflect kind of safety factors in this special case, with a value of 1.2 to 1.4.

For a transient slab uplift computation, the dynamic under pressures without transients are multiplied by this amplification factor. During the preparation of the described analysis the amplification factor was changed to 1.5 to 2.0. This was the result of a discussion with the mentioned researcher who could consider current research results which showed that the safety factors which were recommended in earlier publications were too optimistic.

This increase of the factor shows the highly sensitive load conditions of hydraulic systems such as plunge pools when dealing with dynamic, turbulent flows.

REFERENCES

Bollaert, E.F.R., 2004. A new procedure to evaluate dynamic uplift of concrete linings or rock blocks in plunge pools, *Proc. of the Intl. Conf. Hydraulics of Dams and River Structures*, *Yazdandoost & Attari (eds.)*, Teheran, Iran, pp. 125–132.

Bollaert, E.F.R. & Schleiss, A. 2003. Scour of rock due to the impact of plunging high velocity jets Part I: A state-of-the-art review. *Journal of Hydraulic Engineering*, Vol. 41, No. 5, 451–464.

Bollaert, E.F.R. & Schleiss, A. 2005. Physically Based Model for Evaluation of Rock Scour due to High-Velocity Jet Impact. *Journal of Hydraulic Engineering*, Vol. 131, No. 3, pp. 153–165.

Castillo, L.G. 2006. Aerated Jets and Pressure Fluctuation in Plunge Pools. *The 7th Int. Conference on Hydroscience and Engineering (ICHE-2006)*, Sep 10–13, Philadelphia, USA.

Castillo, L.G.; Carrillo, J.M. 2016. Pressure and Velocity Distributions in Plunge Pools. *2nd International Seminar on Dam Protection Against Overtopping*, Ft. Collins, Colorado, USA, 7–9 September 2016.

Ervine, D.A.; Falvey, H.T.; Withers, W. W. A. 1997. Pressure fluctuations on plunge pool floors. *Journal of Hydraulic Research*, Vol. 35, No. 2, pp. 257–279.

Hager, W.H. & Vischer, D.L. 1995. Energy Dissipators – Hydraulic Design Considerations. *Hydraulic Structures Manual, IAHR AIRH*, A. A. Balkema, Rotterdam Brookfield.

Johnson, P.L. (1974): Hydraulic Model Studies of Plunge Basins for Jet Flow. *U.S. Bureau of Reclamation*, *REC-ERC-74-9*, Denver, Colorado.

Mason, P.J. & Arumugam, K. 1985. Free Jet Scour Below Dams and Flip Buckets. *Journal of Hydraulic Engineering, Vol. 111, No. 2*, ASCE.

May, R.W.P. & Willoughby, I.R. 1991. Impact Pressures in Plunge Basins Due to Vertical Falling Jets. Hydraulic Research, Ltd., *Wallingford, Oxfordshire (UK), Research Report (PECD 7/6/113)*.

Puertas, J. & Dolz, J. 2005. Plunge Pool Pressures Due to a Falling Rectangular Jet. *Journal of Hydraulic Engineering*, Vol. 131, No. 5, pp. 404–407.

Veronese, A. 1937. Erosioni do Fondo a Valle di uni Scarico. *Annali dei Lavori Publicci*, Vol. 75, No. 9, pp. 717–726. Italy.

Wittler, R.J.; Annandale, G.W.; Abt, S.R.; Ruff, J.F. 1998. New Technology for Estimating Plunge Pool or Spillway Scour. *Proceedings of the 1998 Annual Conference of the Association of State Dam Safety Officials*, *October 11–14*. Las Vegas.